Nonlocal Means Denoising of ECG Signals

Brian H. Tracey*, *Senior Member, IEEE*, and Eric L. Miller, *Fellow, IEEE*

***Abstract*—Patch-based methods have attracted significant attention in recent years within the field of image processing for a variety of problems including denoising, inpainting, and super-resolution interpolation. Despite their prevalence for processing 2-D signals, they have received little attention in the 1-D signal processing literature. In this letter, we explore application of one such method, the nonlocal means (NLM) approach, to the denoising of biomedical signals. Using ECG as an example, we demonstrate that a straightforward NLM-based denoising scheme provides signal-to-noise ratio improvements very similar to state of the art wavelet-based methods, while giving $\sim 3\times$ or greater reduction in metrics measuring distortion of the denoised waveform.**

***Index Terms*—Denoising, ECG, nonlocal means.**

I. Introduction

ACCURATE extraction of clinical parameters from noisy biomedical signals is a critical and on-going challenge. Many sources of signal contamination including additive high-frequency noise, motion or muscle artifacts, and baseline wander overlap signals of clinical interest in both time and frequency [1]–[3]. Thus, in the process of removing these sources of contamination, standard filtering approaches can also adversely affect these desired signal components. For example, low-pass filtering may suppress high-frequency noise, and also distorts waveform spikes in electromyography (EMG) or ECG signals [2]. Important advances in biomedical signal denoising have been made, with a large and growing literature on wavelet denoising [1] and other techniques [3], [4].

Denoising is also central to image processing [5]. A key problem here is the need to preserve sharp edges, which often are critical to image interpretation. A recent approach to image denoising which addresses the problem of edge degradation is the nonlocal means filter, introduced by Buades *et al.* [6]. Their work has attracted over 1000 citations and many extensions of the original algorithm have been proposed [7]–[9]. The nonlocal means (NLM) filter, described in the next section, denoises images by averaging patches from different regions in the image but which have similar spatial structure, relying on the fact that natural images often contain repeated patterns. We note that many biomedical signals (ECG being a clear example) have a regular morphology that repeats with slight variations, and therefore may be amenable to patch-based methods. Although a predecessor method has been applied to ECG [10], we are not aware of previous use of NLM for 1-D biomedical signals.

In this letter, we briefly describe the NLM algorithm, and discuss its application in the context of ECG denoising. We present results for ECG denoising of signals with simulated additive noise. Encouragingly, the NLM results are very competitive with recently published wavelet denoising results on the same data [4]. Finally, we discuss some possible directions for future work. While we focus here on ECG data as a first example, NLM denoising should be applicable to a wider range of biomedical signals such as EMG or evoked potentials.

II. Denoising Methods

A. Basic Nonlocal Means Algorithm

Nonlocal means denoising [6] addresses the problem of recovering the true signal $\mathbf{u}$ given a set of noisy observations, $\mathbf{v} = \mathbf{u} + \mathbf{n}$, where $\mathbf{n}$ is additive noise. For a given sample s, the estimate $\hat{u}(s)$ is a weighted sum of values at other points t that are within some "search neighborhood' $N(s)$

$$\hat{u}(s) = \frac{1}{Z(s)} \sum_{t \in N(s)} w(s,t) v(t) \tag{1}$$

where $Z(s) = \sum_t w(s,t)$, and the weights are [7]

$$w(s,t) = \exp\left(-\frac{\sum_{\delta \in \Delta} (v(s+\delta) - v(t+\delta))^2}{2 L_\Delta \lambda^2} \right) \equiv \exp\left(-\frac{d^2(s,t)}{2 L_\Delta \lambda^2} \right) \tag{2}$$

(note [6] defined the denominator above as h^2). In (2), λ is a bandwidth parameter, while Δ represents a local patch of samples surrounding s, containing L_Δ samples; a patch of the same shape also surrounds t. Although a variety of patch weightings are possible [6], [8], square patches centered on the points of interest are most common. In (2) we have defined d^2 to denote the summed, squared point-by-point difference between samples in the patches centered on s and t.

In (2), each patch is averaged with itself with weight $w(s,s) = 1$. To achieve a smoother result, a center patch correction is often applied, i.e.,

$$w(s,s) = \max_{t \in N(s), t \neq s} w(s,t). \tag{3}$$

As discussed below, we chose *not* to apply this correction, to avoid oversmoothing the QRS complex.

The novelty of NLM is that the weighting $w(s,t)$ depends on patch similarity, not on the physical distance between the points s and t. Averaging similar patches helps to preserve edges, in

Manuscript received April 9, 2012; revised June 5, 2012; accepted July 5, 2012. Date of publication July 17, 2012; date of current version August 16, 2012. *Asterisk indicates corresponding author.*

*B. Tracey is with the Department of Electrical and Computer Engineering, Tufts University, Medford, MA 02155 USA (e-mail: brian.tracey@tufts.edu).

E. L. Miller is with the Department of Electrical and Computer Engineering, Tufts University, Medford, MA 02155 USA (e-mail: elmiller@ece.tufts.edu).

Color versions of one or more of the figures in this paper are available online at http://ieeexplore.ieee.org.

Digital Object Identifier 10.1109/TBME.2012.2208964

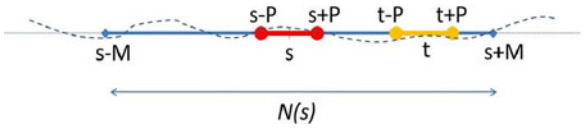

Fig. 1. Illustration of NLM parameters. The small patch centered on s is compared to patches centered on other points t in $N(s)$.

contrast to more typical filtering (cf., convolution by a Gaussian smoothing kernel). Assuming self-similarity extends throughout the signal, the neighborhood $N(s)$ is ideally taken to be the entire signal, so the averaging process is fully *nonlocal*. However, the computation scales linearly with the size of $N(s)$, so $N(s)$ is usually limited to reduce computation.

Significant effort has been devoted to fast NLM methods, for example using principle components analysis for dimensionality reduction [11], [12]. For all results (see Section III), we use a fast NLM method proposed by Darbon *et al.* [9]. This approach significantly speeds NLM by reordering operations to eliminate a nested loop. For a 1-D signal of length N, the computational complexity of [9] is $O(2NM)$ versus $O(L_\Delta NM)$ for the Buades algorithm.

B. Parameter Selection

Here, we examine parameter selection for ECG denoising. The key NLM parameters are the patch size, specified as a half-width P (so $L_\Delta = 2P + 1$), the size of $N(s)$, specified as a half-width M, and the bandwidth λ. Fig. 1 shows the geometric parameters schematically, for 1-D patches centered on the points s and t.

The *bandwidth* λ is a key parameter that controls the amount of smoothing applied. An overly small λ will cause noise fluctuations to have too much influence in deweighting different patches, resulting in insufficient averaging; an overly large λ will cause dissimilar patches to appear similar, resulting in blur. Ville and Kocher in [7] used the SURE criterion for parameter selection and noted that for their test set, a good overall choice of lambda is 0.5 σ, where σ is the noise standard deviation. It is intuitive that λ should scale by σ, as for a locally flat area, $d^2 \sim 2\sigma^2$, as variances add. Interestingly, our results below for ECG denoising find a result very similar to [7].

The *patch half-width* P selects the scale on which patches are compared, and should generally be similar to the size of features of interest. For ECG signals, a reasonable choice for P is the half-width of the high-amplitude "*R*" ECG complex.

In principle, increasing the *neighborhood half-width* M (resulting in a "less local" search) should lead to better performance. However, a larger search window maps directly to increased computation, even in the case of the fast algorithms described earlier. For ECG denoising of the QRS complex, setting M large enough to include multiple heartbeats allows multiple QRS regions with potentially similar morphology to be compared. Note that the shape of high-amplitude QRS regions is naturally protected, as differences between even visually similar peaks are typically large ($\gg\lambda$), resulting in low weights and thus little smoothing of these regions.

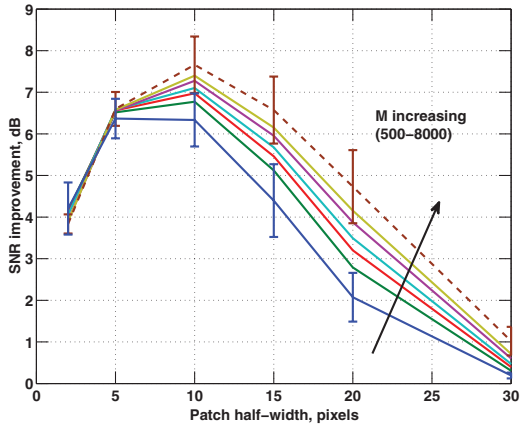

Fig. 2. SNR improvement (dB) versus P and M ($\lambda = 0.6\sigma$). Each curve corresponds to a value of M, with the arrow showing direction of increase. Errorbars (top and bottom curves only, for clarity) show standard deviation across the set of waveforms.

III. Results

For simulations, we use data from the Physionet MIT-BIH arrythmia database (www.physionet.org), for the ECG signals numbered as 100, 103, 104, 105, 106, 115, and 215. These recordings were sampled at 360 Hz using 11-bit A/D converters. We processed both the actual Physionet recordings (converted to milli volts) and the signals with the white Gaussian noise added to achieve target signal-to-noise ratio (SNR) levels. The signals chosen and SNR levels used in simulation are identical to those used in [4] allowing us to compare NLM to their results.

Following [4], we quantify denoising performance in terms of SNR improvement ($\mathrm{SNR}_{\mathrm{imp}}$) in decibel, mean squared error (MSE), and percent distortion (PRD)

$$\mathrm{SNR}_{\mathrm{imp}} = 10\log_{10}\frac{\sum_{n=1}^{N}(v[n]-u[n])^2}{\sum_{n=1}^{N}(\hat{u}[n]-u[n])^2}$$

$$\mathrm{MSE} = \frac{1}{N}\sum_{n=1}^{N}(\hat{u}[n]-u[n])^2$$

$$\mathrm{PRD} = 100\sqrt{\frac{\sum_{n=1}^{N}(\hat{u}[n]-u[n])^2}{\sum_{n=1}^{N}u^2[n]}} \tag{4}$$

where N is the signal length in samples and u and v are as described earlier. Note that here we are assuming the Physionet signals are the true signals u; in reality these signals also contain noise, which the metrics above neglect, though at most SNRs the (simulated) additive noise dominates. These metrics and approach are borrowed from [4] to facilitate comparison to their results.

We performed parameter tuning based on the first Physionet waveform ensemble and found good performance for $P = 10$ samples, $M \geq 2000$ samples, and $\lambda \approx 0.6\sigma$ (in our simulated data the noise variance σ^2 is known; in practice it can be estimated from data or system characteristics). Figs. 2 and 3 motivate these choices. Fig. 2 shows the calculated SNR improvement for a 10-dB SNR signal, with $\lambda = 0.6\sigma$, and varying P and M. $\mathrm{SNR}_{\mathrm{imp}}$ is sensitive to the patch size, with best

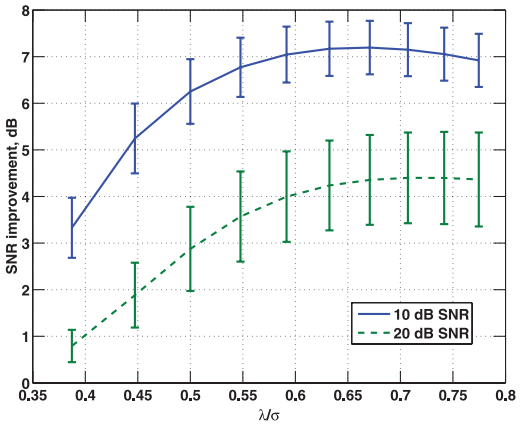

Fig. 3. SNR improvement versus λ ($P = 10$, $M = 2000$); errorbars show standard deviation across the set of waveforms.

results near $P = 10$ samples, giving a 21-sample (58-ms duration) patch. This duration matches well with typical widths of the high-amplitude ECG signal portion. $\mathrm{SNR}_{\mathrm{imp}}$ improves monotonically with M, but the improvement slows with larger M. Results are good for $M \geq 2000$, which corresponds to a window of roughly ten heartbeats. Fig. 3 shows $\mathrm{SNR}_{\mathrm{imp}}$ as function of λ/σ for several SNRs. Best results are obtained for λ/σ around 0.6. Both figures show errorbars that indicate the standard deviation across the ensemble of waveforms.

Fig. 4 shows ECG signal 100, showing original data (top), denoised data (middle), and the signal with noise added to achieve 10-dB SNR (bottom). This high-noise signal is shown both before and after NLM denoising is applied. For the simulated signal, λ is chosen based on the known noise variance; for the raw Physionet signal, λ was chosen by inspection (as 1/5 of the 10-dB value). In both cases $P = 10$ and $M = 2000$. Both the actual signals and the signal with added noise are seen to be smoothed by NLM filtering. A noteworthy aspect, discussed below, is that the high-amplitude signal regions are nearly unaffected by denoising.

Finally, Fig. 5 shows all three metrics calculated across the full dataset as a function of SNR. The Figure also shows results for two algorithms presented in [4]; a wavelet soft thresholding algorithm (with threshold learned from a training set), and a hybrid empirical mode decomposition/wavelet denoising method (values are taken from figures in [4]). NLM achieves lower signal distortion than the other methods, reducing MSE by ∼3–14×. NLM gives very similar $\mathrm{SNR}_{\mathrm{imp}}$ to the other methods, particularly at the higher SNRs more similar to the Physionet data.

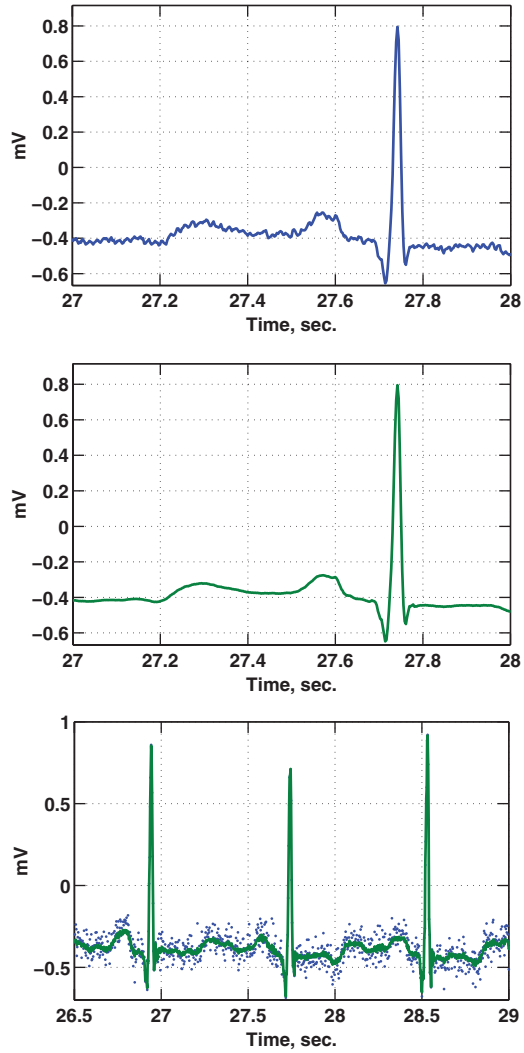

Fig. 4. ECG waveform 100; raw data (top), denoised (middle), and signal with 10-dB SNR added noise, before and after denoising (bottom).

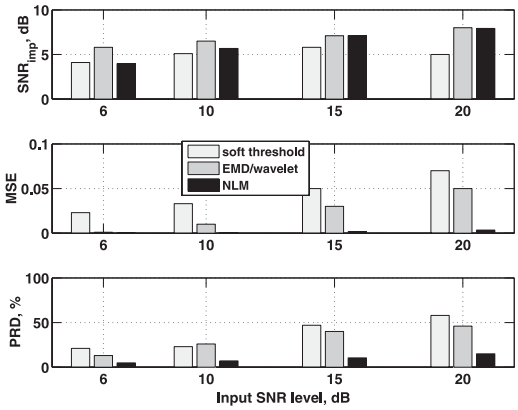

Fig. 5. Performance metrics, averaged across the full dataset.

IV. Discussion

We have shown that a straightforward application of NLM to ECG denoising gives SNR improvements competitive with state-of-the-art wavelet denoising while causing noticeably less signal distortion. We next discuss some limitations and possible extensions of the method.

Here we have applied NLM to denoising of ECGs with additive white Gaussian noise. While this denoising problem is of interest [4], other ECG denoising schemes have focused on more structured artifacts such as those caused by motion or muscle activity [3]. The basic NLM approach of looking for signal patches with similar characteristics is likely to be less

successful in suppressing interference artifacts. However, NLM could be combined with interference rejection methods, as is done with other techniques [2]. NLM could also prove useful in denoising evoked potential recordings, where additive noise is a significant problem that is typically addressed through signal averaging.

As noted earlier, NLM had little effect on the morphology of the high-amplitude portions of the ECG signal. This can be explained intuitively, as even small variations in the shape of high-amplitude signal patches centered on s and t can lead to a large difference $d^2(s,t)$, and thus to very low weights. Thus, while lower amplitude portions of the signal have many similar patches, we found that the high-amplitude signal regions do not match other regions well and therefore are very lightly averaged (here, it is important that we do *not* apply (3), instead allowing each center patch to fully contribute to the output). This phenomenon is closely related to the "rare patch" concept noted in NLM image denoising [8]. In the ECG application, this "rare patch" effect can be beneficial; it means that denoising is focused on low-amplitude signal regions, which are naturally low SNR and therefore benefit most from denoising, while high-SNR signal regions are less affected. However, a disadvantage is that signal regions that are near a high-amplitude region, but not part of it, may be under averaged so that signal takeoffs are not as clear as desired. Several solutions to this problem exist, for example, locally adaptive bandwidth parameter selection [7], shape-adaptive patches [8], or their combination [12] and may provide promising avenues for future work.

V. Conclusion

In this letter, we have applied a 1-D implementation of the nonlocal means denoising algorithm, which has received significant attention in image processing, to denoising of ECG signals. The results are promising, suggesting the method can provide denoising while minimizing signal distortion. We have noted some limitations of the method and suggest possible avenues for the application and improvement of the technique. Given the success of patch-based methods in image processing, we are optimistic that NLM and related methods may be useful in denoising biomedical signals.

Acknowledgment

The authors gratefully acknowledge the insightful comments of the reviewers.

References

[1] P. S. Addison, "Wavelet transforms and the ECG: A review," *Physiol. Meas.*, vol. 26, no. 5, pp. R155–R199, 2005.

[2] M. Blanco-Velasco, B. Weng, and K. E. Barner, "ECG signal denoising and baseline wander correction based on the empirical mode decomposition," *Comput. Biol. Med.*, vol. 38, no. 1, pp. 1–13, 2008.

[3] T. He, G. Clifford, and L. Tarassenko, "Application of independent component analysis in removing artefacts from the electrocardiogram," *Neural Comput. Appl.*, vol. 15, no. 2, pp. 105–116, 2006.

[4] M. Kabir and C. Shahnaz, "Denoising of ECG signals based on noise reduction algorithms in EMD and wavelet domains," *Biomed. Signal Process. Control*, vol. 7, no. 5, pp. 481–489, 2012.

[5] R. C. Gonzalez and R. E. Woods, *Digital Image Processing*, 3rd ed. Englewood Cliffs, NJ: Prentice-Hall, Aug. 2007.

[6] A. Buades, B. Coll, and J. M. Morel, "A review of image denoising algorithms, with a new one," *Multiscale Modeling and Simulation*, vol. 4, no. 2, pp. 490–530, 2005.

[7] D. Van De Ville and M. Kocher, "SURE-based nonlocal means," *IEEE Signal Process. Lett.*, vol. 16, no. 11, pp. 973–976, Nov. 2009.

[8] C. A. Deledalle, V. Duval, and J. Salmon, "Nonlocal methods with shape-adaptive patches (NLM-SAP)," *J. Math. Imag. Vis.*, vol. 43, no. 2, pp. 103–120, 2012.

[9] J. Darbon, A. Cunha, T. F. Chan, S. Osher, and G. J. Jensen, "Fast nonlocal filtering applied to electron cryomicroscopy," in *Proc. 5th IEEE Int. Symp. Biomed. Imag.*, 2008, pp. 1331–1334.

[10] D. Shih, H. Chiang, S. Lin, and M. Shih, "An intelligent ECG reasoning system for the elderly," in *Proc. IEEE Conf. Mach. Learn. Cybern.*, 2007, vol. 4, pp. 1826–1831.

[11] T. Tasdizen, "Principal neighborhood dictionaries for nonlocal means image denoising," *IEEE Trans. Image Proc.*, vol. 18, no. 12, pp. 2649–2660, Dec. 2009.

[12] D. Van De Ville and M Kocher, "Nonlocal means with dimensionality reduction and SURE-based parameter selection," *IEEE Trans. Image Proc.*, vol. 20, no. 1, pp. 1732–1735, Sep. 2011.